

Scalar-product cluster variation method layer formulation for the irregular tetrahedron cluster in bcc lattices

Cláudio Geraldo Schön^{1,*} and Ryoichi Kikuchi²¹*Computational Materials Science Laboratory, Department of Metallurgical and Materials Engineering, Escola Politécnica da Universidade de São Paulo, CEP 05508-900 São Paulo, São Paulo, Brazil*²*University of California at Berkeley, Berkeley, California, USA*

(Received 23 May 2005; revised manuscript received 20 July 2005; published 6 September 2005)

The scalar-product cluster variation method (SP-CVM) for calculation of antiphase boundary (APB) energies has been extended for application to $\{001\}$ APBs in the body-centered cubic lattice using the irregular tetrahedron cluster approximation. In order to do so, the proof of the SP-CVM relation has been updated to include the cases where the domain interface consists of more than one plane of atoms (i.e., it consists of a layer of atoms). The algorithm has been developed for the cases of thermal APBs with APB vectors $a_0^{A2}\langle 100 \rangle$ and $a_0^{A2}/2\langle 111 \rangle$. It is then applied, as an illustration, to the determination of APB energies in isothermal calculations in the Fe-Al system.

DOI: [10.1103/PhysRevB.72.094101](https://doi.org/10.1103/PhysRevB.72.094101)

PACS number(s): 61.72.Bb, 05.70.Np, 64.60.Cn, 81.05.Bx

I. INTRODUCTION

Domain interfaces, like antiphase boundaries (APBs) and magnetic domain boundaries (MDBs), are typical crystal defects of ordered systems (alloy superlattices for the former and ferro- or antiferromagnetic systems for the latter). These defects control important macroscopic properties of technological materials, e.g., plastic deformation behavior (both strength and ductility) of iron aluminides^{1,2} and hysteretic losses in electrical steels.³ The understanding of APB and MDB energetics is, therefore, essential in the design of new advanced ordered materials with optimized properties.

From the theoretical perspective, APBs may be handled within two limit boundary conditions for the sake of studying the defect's energetics.⁴ Defects subjected to the first boundary condition, denoted *mechanical APBs*, are formed under the constraint that the configuration near the plane of the defect remains the same as in a virtual nondefective crystal at the same temperature and alloy composition (denoted the "bulk" configuration). In the second case the defects are denoted *thermal APBs*, and, contrary to the previous one, full local equilibrium is assumed to be established at the interface between the ordered domains, i.e., the configurations near the APB plane *differ* from the bulk.

In the case of mechanical APBs, the constrained equilibrium allows one to treat the problem disregarding the variation of the configurational entropy produced in the system by the introduction of the defect. The defect's specific energy, σ^α (i.e., the APB surface tension for the α th defect type, where α is a short representation of both its plane and vector) is, thus, simply calculated as the variation of the system's internal energy per unit area of defect. The internal energy of ordered systems is usually treated by the Ising model, which attributes a "bond" energy to pairs or other groups of atoms (for a discussion on the theoretical background of the applicability of the Ising model to configurational ordering in alloy systems, see, for example, Bieber and Gautier⁵). In this case the evaluation of the internal energy variation is determined by counting the bonds which are broken by the intro-

duction of the defect, subtracting them from those which are restored in the same process. This procedure is called the *bond counting* (BC) method, which has been successfully applied to the evaluation of APB energies in a large number of systems.^{4,6-9} Mechanical APBs are expected to be produced in alloys mainly as a consequence of plastic deformation and dislocation slip.⁹

The relaxation in the configurations near the plane of the defect in thermal APBs, on the other hand, requires the evaluation of the configurational entropy variation. The APB surface tension is, thus, proportional to the variation of the excess free energy produced by the introduction of the defect in the system. This has to be minimized at the APB interface, subject to asymptotic boundary values corresponding to fixed bulk configurations at infinite distances from the APB plane.^{10,11} The methods used for the calculation of thermal APB energies are, therefore, considerably more complex in comparison with the BC method, since at least one additional minimization step is needed for the evaluation of this excess free energy. Two of these methods will now be briefly reviewed.

A. Methods for the calculation of thermal APB energies

The use of flexible theoretical methods, capable of extension to multicomponent systems and of delivering results within reasonable CPU times and using limited computation resources, is imperative in the framework of computational thermodynamics, since this discipline is, in principle, dedicated to modeling technological materials for industrial process control.^{12,13} One of the theoretical methods which presents this characteristics is the cluster variation method (CVM).¹⁴ Within the CVM two alternative formalisms have been developed by one of the present authors to calculate the excess free energy of thermal APBs in crystal systems: the sum method (S-CVM),^{10,15} and the scalar product method (SP-CVM).^{11,16-19} In the S-CVM the 3D crystal is subdivided into a set of planes parallel to the APB, and the CVM equations are

solved separately for each plane, subject to compatibility constraints with the neighbors.^{10,15} This method allows the detailed calculation of the configuration gradient of the system as a function of the distance from the APB plane, but requires the use of considerable computational resources. In fact, the determination of the local equilibrium configuration *for each plane* depends on the solution of a nonlinear equation system with dimensions of the same order as the one used for a single equilibrium CVM calculations (denoted here as a “bulk” calculation). The S-CVM is also prone to finite-size effects, since the number of planes considered in the implementation of the algorithm must necessarily remain finite. This requires that the asymptotic boundary conditions (corresponding in principle to planes located at infinite distances from the APB) must be imposed both for the first and for the last plane included in the particular implementation, which becomes a better approximation as the size of the system (i.e., the number of planes) increases.

The second method, SP-CVM, is based on ideas developed by Woodbury and Clayton,^{20–22} and adapted by one of the present authors for the application within the CVM formalism.^{11,16–19} This method circumvents the evaluation of the full configuration gradient of the system in the calculation of the excess free energy produced by the defect. It is, thus, considerably simpler to apply, producing faster algorithms compared with the analogous S-CVM formulation. The asymptotic boundary conditions are explicitly used in the SP-CVM theoretical framework as limits for infinite distances from the APB plane and no length scale perpendicular to the APB plane is required in the calculation. The SP-CVM, therefore, is not subject to finite-size effects.

Despite the technological importance of the problem of determination of excess free energies for thermal APBs, only considerably simple cluster approximations and lattice geometries have been investigated to date using either the S-CVM or SP-CVM calculations.

The present work aims to apply the SP-CVM method to the investigation of {001} APB energies in the body-centered cubic (bcc) lattice using the irregular tetrahedron (IT) cluster approximation. This approximation allows one to treat technological materials like iron aluminides^{23,24} and high-spin ferromagnetic systems.^{25,26} The application of the method to a more complex lattice and cluster approximation than those used in previous investigations¹⁹ requires the generalization of the formalism (Sec. II), with a consequent need to update the proof of the basic relation of the SP-CVM method. This will also be discussed in the present work (Sec. II A). The use of the algorithm will be illustrated by calculations in the Fe-Al system (Sec. III), which has been chosen as a prototype system for the calculations due to the existence of reliable phenomenological parameters,^{23,24} which reproduce both the phase diagram topology of iron-rich alloys and aluminum activity measurements at $T=1000$ K.²⁷ For simplicity’s sake, the present calculations will be limited to the so called “nonmagnetic” Fe-Al system (i.e., the effect of the spin orientations of the iron atoms will be neglected in building the thermodynamic model). The formalism may be, however, immediately extended to treat magnetic cases and mixed chemical-magnetic cases using the Ising model to describe the magnetic interactions.²⁸ Finally the results will be discussed in Sec. IV.

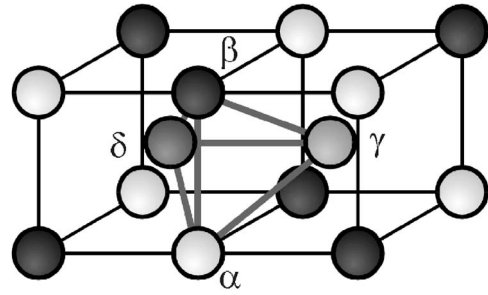


FIG. 1. The irregular tetrahedron (IT) cluster in the bcc lattice.

II. SCALAR PRODUCT-CLUSTER VARIATION METHOD IN THE “LAYER” FORMULATION

The scalar product method receives its name from the basic relation, derived by Clayton and Woodbury^{20–22}

$$\exp\left(-\frac{A\sigma^\alpha}{k_B T}\right) = \sum_{\mu} [p^I(\mu)p^{II}(\mu)]^{1/2}. \quad (1)$$

In the expression above, $A=N(a_0^{A2})^2$ represents the area of the {001} interface with N atoms (with a_0^{A2} being the lattice parameter of a disordered bcc lattice, $A2$), $k_B=8.3145$ J mol⁻¹ K⁻¹ is Boltzmann’s constant, T the absolute temperature, and σ^α the surface tension for the α th APB, to be determined. The sum on the right-hand side runs over all configurations of the interface (represented collectively by the symbol μ) and $p^{I,II}$ corresponds to the conditional probability of finding this particular configuration in the “bulk” crystal at domains I and II, respectively. The right-hand side of Eq. (1) resembles the definition of a scalar product in a vector space (e.g., \mathbb{R}^n), hence the name of the method.

CVM-related concepts are used in the scalar product method to evaluate probabilities p^I and p^{II} , based on equilibrium bulk CVM calculations, and to solve the nonlinear set of equations corresponding to Eq. (1).

Figure 1 shows the irregular tetrahedron cluster used to model the thermodynamics of the bcc lattice. Analyzing this figure, it becomes clear that the cluster depicted in it is built by atoms belonging to three {001} atom planes, say at coordinates 0.0 , $0.5a_0^{A2}$ and $1.0a_0^{A2}$ along the [001] axis. The configuration corresponding to the interface thus cannot be described by a single pair of atom planes, as in the previous formulations of the SP-CVM.^{11,16–19} In the present case, it is necessary to consider at least a layer composed by two consecutive [001] atom planes to describe the interface configuration. The existing proofs for the validity of Eq. (1) (see, e.g., Cenedese and Kikuchi¹¹) have been, however, derived under the assumption that the interface is formed by a single atomic plane. This proof must be, therefore, updated for the present layer formulation. This will be done next, before returning to the particular implementation of the algorithm for the case of the IT cluster.

A. Proof for the validity of the scalar product relation in the “layer” formulation

Figure 2 represents the [010] projection of a bcc crystal block, with the layer construction used for the evaluation of

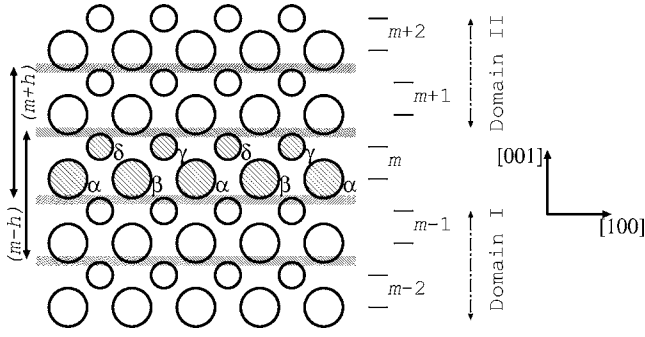


FIG. 2. Schematic [010] projection of a bcc crystal showing the layer construction for the evaluation of (001) APB energies using the S-CVM. Small circles represent atoms which are located half a lattice parameter below the plane of the figure. The APB is placed in the layer denoted by “ m ,” which is the intersection of the layer pairs centred at $m+h$ and $m-h$ ($h=\frac{1}{2}$).

the energy of a domain interface located at plane (001) in a hypothetical S-CVM formulation of the problem. The domain interface is, by definition, located at the layer denoted “ m ,” which is at the intersection of the layer pair centered at $m+h$ ($h=\frac{1}{2}$) and the one centered at $m-h$ (both are also shown in the figure).

We introduce the variables $p(m, \mu)$ and $q(m+h, \mu, \nu)$ as the probability to find layer m with configuration μ and of finding the layer pair $m+h$ with configuration μ at m and ν at $m+1$. Since the configuration gradient must be continuous in any case, these probabilities must be related by

$$p(m', \nu) = \sum_{\mu} q(m' - h, \mu, \nu) = \sum_{\xi} q(m' + h, \nu, \xi). \quad (2)$$

Also, the layer pair probabilities must be normalized [this ensures, by Eq. (2), that the layer probabilities are normalized as well]

$$\sum_{\mu} \sum_{\nu} q(m' + h, \mu, \nu) = 1. \quad (3)$$

We denote the interaction energy of a layer pair as $\varepsilon(\mu, \nu)$. This quantity is composed of layer self-energies (i.e., the energy of the bonds contained in a single layer), $\varepsilon_1(\mu)$, and a layer interaction energy, $\varepsilon_2(\mu, \nu)$ (i.e., due to the bonds which belong to both layers)

$$\varepsilon(\mu, \nu) = \varepsilon_2(\mu, \nu) + \frac{\varepsilon_1(\mu) + \varepsilon_1(\nu)}{2}. \quad (4)$$

The internal energy of the entire system is expressed as

$$U = \sum_m \sum_{\mu} \sum_{\nu} \varepsilon(\mu, \nu) q(m+h, \mu, \nu). \quad (5)$$

The entropy of the system is written in terms of the layer pair probabilities as

$$S = -k_B \left\{ \sum_m \sum_{\mu} \sum_{\nu} q(m+h, \mu, \nu) \ln q(m+h, \mu, \nu) - \frac{1}{2} \left[\sum_{\mu} p(m, \mu) \ln p(m, \mu) + \sum_{\nu} p(m+1, \nu) \ln p(m+1, \nu) \right] \right\}. \quad (6)$$

The expression above can be obtained considering that the problem is topologically equivalent to the unidimensional lattice in the pair approximation, whose solution is found, for example, in Kikuchi (1951).¹⁴

The Helmholtz free energy, F , of the crystal is written as

$$F = U - TS + C_{\alpha} + C_{\lambda}, \quad (7)$$

where C_{α} and C_{λ} are the constraint terms introduced to ensure the validity of Eqs. (2) and (3). These are defined in terms of the layer pair probabilities as

$$\begin{aligned} C_{\alpha} &\equiv k_B T \sum_m \sum_{\nu} \alpha(m, \nu) \left[\left(\sum_{\mu} q(m-h, \mu, \nu) \right) - \left(\sum_{\xi} q(m+h, \nu, \xi) \right) \right] \\ &= \sum_m \sum_{\mu} \sum_{\nu} [\alpha(m+1, \nu) - \alpha(m, \mu)] q(m+h, \mu, \nu), \end{aligned} \quad (8)$$

and

$$C_{\lambda} \equiv \sum_m \lambda(m+h) \left[1 - \left(\sum_{\mu} \sum_{\nu} q(m+h, \mu, \nu) \right) \right], \quad (9)$$

with $\alpha(m', \xi)$ and $\lambda(m'+h)$ being the corresponding Lagrange multipliers.

Differentiating Eq. (7) relative to $q(m+h, \mu, \nu)$, equating to zero, and rearranging the terms, one obtains

$$q(m+h, \mu, \nu) = \exp \left[\frac{\lambda(m+h) - \varepsilon(\mu, \nu)}{k_B T} \right] [p(m, \mu) p(m+1, \nu)]^{1/2} \exp[\alpha(m, \mu) - \alpha(m+1, \nu)]. \quad (10)$$

This defines an implicit function for $q(m+h, \mu, \nu)$, with the Lagrange multipliers being determined using the respective constraints. Equation (10) has a solution for a set of fixed points in the $q(m+h, \mu, \nu)$ space. These fixed points correspond to local equilibrium values for the constrained equilibrium states for the inhomogeneous system, which can be found by a simple self-consistent algorithm (the “natural iteration method,” NIM), previously introduced by one of the present authors.²⁹ The NIM algorithm is very robust and, for some cases (including the 1D lattice in the pair approximation), it has been proved that it always converges to a solution in the form of a stable (or, at least metastable) fixed point.³⁰ After the convergence to a fixed point in the layer pair probability space, F may be obtained from the Lagrange multipliers by:

$$F = \sum_m \lambda(m+h). \quad (11)$$

We introduce now the following auxiliary functions:

$$\begin{cases} f(m, \eta) = p(m, \eta)^{1/2} \exp[+\alpha(m, \eta)], \\ g(m, \eta) = p(m, \eta)^{1/2} \exp[-\alpha(m, \eta)], \\ \Lambda(\eta, \xi) = \exp\left[-\frac{\varepsilon(\eta, \xi)}{k_B T}\right]. \end{cases} \quad (12)$$

With their help we are able to rewrite Eq. (10) in a more compact form

$$q(m+h, \mu, \nu) = \exp\left[\frac{\lambda(m+h)}{k_B T}\right] f(m, \mu) \Lambda(\mu, \nu) g(m+1, \nu). \quad (13)$$

Substituting Eq. (13) into Eq. (2), performing the summations, and using the identity $p(m, \mu) \equiv f(m, \mu)g(m, \mu)$, we obtain

$$f(m, \nu) = \exp\left[\frac{\lambda(m-h)}{k_B T}\right] \sum_{\mu} \Lambda(\mu, \nu) f(m-1, \mu), \quad (14a)$$

$$g(m, \nu) = \exp\left[\frac{\lambda(m+h)}{k_B T}\right] \sum_{\xi} \Lambda(\nu, \xi) g(m+1, \xi). \quad (14b)$$

We apply now Eq. (13) for two arbitrary layers, m' and m'' , and first sum over ν , using Eq. (14b), then over μ , using Eq. (14a), obtaining

$$\begin{aligned} & \sum_{\mu} \sum_{\nu} f(m', \mu) \Lambda(\mu, \nu) g(m''+1, \nu) \\ &= \sum_{\mu} f(m', \mu) \exp\left[-\frac{\lambda(m''+h)}{k_B T}\right] g(m'', \mu) \\ &= \sum_{\nu} f(m'+1, \nu) \exp\left[-\frac{\lambda(m'+h)}{k_B T}\right] \\ & \quad \times g(m''+1, \nu). \end{aligned} \quad (15)$$

Finally, we obtain the *recursion relation*

$$\begin{aligned} & \sum_{\mu} f(m', \mu) g(m'', \mu) \\ &= \exp\left[\frac{-\lambda(m'+h) + \lambda(m''+h)}{k_B T}\right] \sum_{\mu} f(m'+1, \mu) \\ & \quad \times g(m''+1, \mu). \end{aligned} \quad (16)$$

We chose now $m' = -k$ and $m'' = k$, and iterate the recursion relation $M \geq 2k$ times, obtaining

$$\begin{aligned} & \sum_{\mu} f(-k, \mu) g(+k, \mu) \\ &= \exp\left[\frac{1}{k_B T} \left(\sum_{m''=k}^{k+M} \lambda(m''+h) - \sum_{m'=-k}^{M-k} \lambda(m'+h) \right)\right] \\ & \quad \times \sum_{\mu} f(M-k+1, \mu) g(M+k+1, \mu). \end{aligned} \quad (17)$$

We now place the APB between layers k and $-k$ and choose a large enough value for k such that the layer configurations approach the asymptotic boundary values [i.e., $p(+k, \mu) \approx p^{\text{II}}(\mu)$ and $p(-k, \mu) \approx p^{\text{I}}(\mu)$]. We observe that, by their definition, the summation limits are such that $(M+k) > k$ and $(M-k) > k$, i.e., the summation on the left-hand side of Eq. (17) is performed exclusively well inside domain II (i.e., in the bulk crystal), while the summation on the right-hand side of Eq. (17) is performed across the interface. Taking the limits for large M and k , the terms which depend on the probabilities reduce, therefore, to

$$\lim_{M > 2k \rightarrow \infty} \sum_{\mu} f(-k, \mu) g(+k, \mu) = \sum_{\mu} [p^{\text{I}}(\mu) p^{\text{II}}(\mu)]^{1/2}, \quad (18)$$

and

$$\begin{aligned} & \lim_{M > 2k \rightarrow \infty} \sum_{\mu} f(M-k+1, \mu) g(M+k+1, \mu) \\ &= \sum_{\mu} [p^{\text{II}}(\mu) p^{\text{I}}(\mu)]^{1/2} \\ & \equiv 1. \end{aligned} \quad (19)$$

In deducing Eq. (19), use was made of the translational invariance of the bulk crystal to set $\alpha(m, \mu) = 0$. Considering now the terms which depend on the Lagrange multipliers, we observe that, by definition, $\lambda(P+h) = \lambda^{(0)} (\forall P \geq k)$, where $\lambda^{(0)}$ is the free energy per layer of the bulk crystal; therefore, we can rewrite the term inside the square brackets as

$$\sum_{m''=k}^{k+M} \lambda(m''+h) - \sum_{m'=-k}^{M-k} \lambda(m'+h) = \sum_{m'=-k}^{M-k} [\lambda^{(0)} - \lambda(m'+h)], \quad (20)$$

and finally, taking the limits for $k \rightarrow \infty$ and remembering that $M > 2k$ (i.e., $-k \rightarrow -\infty$ and $M-k \rightarrow +\infty$)

$$\sum_{m''=-\infty}^{+\infty} \lambda^{(0)} - \lambda(m''+h) = -(F - F^{(0)}), \quad (21)$$

where $F^{(0)}$ represents the free energy of the defect-free crystal. From the definition of the defect's surface tension, however, we have

$$\sigma^{\alpha} A \equiv F - F^{(0)}. \quad (22)$$

Substituting Eqs. (18)–(22) into Eq. (17), we obtain Eq. (1), which proves the SP-CVM fundamental relation.

B. Implementation of the SP-CVM layer formulation

The IT cluster partitions the basic bcc lattice into four sublattices, labeled α , β , γ , and δ , respectively (see Fig. 1). The occupancies of these sublattices by the n different species of the system define the ordered states in alloy superlattices⁹ and in ferro- or antiferromagnetic systems.²⁶ A **cluster configuration** is defined by the set $\{i, j, k, l\}$, which corresponds to species i sitting on lattice position α , species j sitting on lattice position β , and so on.⁴⁰

We define the tetrahedron cluster densities $\rho_{i,j,k,l}^{\alpha\beta\gamma\delta}$ by the relation

$$\rho_{i,j,k,l}^{\alpha\beta\gamma\delta} = \frac{N_{i,j,k,l}^{\alpha\beta\gamma\delta}}{N^{\alpha\beta\gamma\delta}}, \quad (23)$$

where $N_{i,j,k,l}^{\alpha\beta\gamma\delta}$ and $N^{\alpha\beta\gamma\delta}$ correspond, respectively, to the number of tetrahedron clusters with configuration $\{i,j,k,l\}$ and the total number of clusters in the system. In the thermodynamic limit ($N^{\alpha\beta\gamma\delta} \rightarrow \infty$) the set $\{\rho_{i,j,k,l}^{\alpha\beta\gamma\delta}\}$ corresponds to a discrete probability distribution, and, for simplicity's sake, these variables will be denominated "tetrahedron cluster probabilities" from now on.

Subcluster probabilities may be defined similarly, but these variables are linearly dependent on the tetrahedron cluster probabilities by the so-called "reduction relations".¹⁴ As an example of a reduction relation, the $\alpha\beta\delta$ triangle probability is given by

$$\rho_{ijl}^{\alpha\beta\delta} = \sum_{k'=1}^n \rho_{ijk'l}^{\alpha\beta\gamma\delta}. \quad (24)$$

As Inden and Pitsch demonstrated,³¹ the independent variables in a CVM calculation can be chosen as corresponding to the tetrahedron cluster probabilities due to this linear dependence.

Using the definition of the IT cluster and of its subclusters, Eq. (1) may be rewritten as

$$\exp\left[\frac{-A\sigma^\alpha}{k_B T}\right] = \sum_{ijkl} \Omega_{ijkl}(\{\rho_{ijkl}^{\alpha\beta\gamma\delta}\}) [P^I(\{\rho_{ijkl}^{\alpha\beta\gamma\delta}\}) P^{II}(\{\rho_{ijkl}^{\alpha\beta\gamma\delta}\})]^{1/2}, \quad (25)$$

where $\{\rho_{ijkl}^{\alpha\beta\gamma\delta}\}$ refers to the local probability distribution of IT clusters at the interface (i.e., at layer m in the notation of Sec. II A) and Ω_{ijkl} is a weight factor for configuration $\{i,j,k,l\}$, defined by the identity

$$\Omega(\{\rho_{ijkl}^{\alpha\beta\gamma\delta}\}) \equiv \prod_{ijkl} \Omega_{ijkl}, \quad (26)$$

with Ω representing the number of configurations of the layer compatible with the probability distribution $\{\rho_{ijkl}^{\alpha\beta\gamma\delta}\}$.

Factor Ω_{ijkl} may be expressed in terms of $\{\rho_{ijkl}^{\alpha\beta\gamma\delta}\}$ using the relation between Ω and the layer configurational entropy, S_ℓ

$$\exp\left[\frac{S_\ell}{k_B}\right] = \frac{\{nn\ pair\}_N^4}{\{point\}_N^2 \{IT\}_N^2} = \Omega. \quad (27)$$

In the previous expression, $\{\xi\}_N$ represents a short notation for the product of the factorials of the number of clusters ξ in a bcc system of N lattice points

$$\{\xi\}_N \equiv \prod_{\{r\}} N_r^\xi! \equiv \prod_{\{r\}} (N\rho_r^\xi)!, \quad (28)$$

where the symbol " $\{r\}$ " represents, schematically, the set of configurations of cluster ξ . The expression for S_ℓ may be derived by different procedures, e.g., using the correlation correction function (CCF) method, recently introduced by one of the present authors (see the Appendix).³²

Finally, the expression for Ω_{ijkl} is obtained by grouping the product terms which correspond to the same set of indices in Eq. (27) and then comparing with Eq. (26).

The expressions of P^I and P^{II} are written in terms of the tetrahedron cluster probabilities in a similar way, using the superposition approximation^{11,17,19,33}

$$\begin{aligned} P^I(\{\rho_{ijkl}^{\alpha\beta\gamma\delta}\}) &= \prod_i (\bar{\rho}_i^{\alpha,1})^{N\rho_i^\alpha/2} \prod_j (\bar{\rho}_j^{\beta,1})^{N\rho_j^\beta/2} \prod_k (\bar{\rho}_k^{\gamma,1})^{N\rho_k^\gamma/2} \\ &\times \prod_l (\bar{\rho}_l^{\delta,1})^{N\rho_l^\delta/2} \prod_{ijkl} (\bar{\rho}_{ijkl}^{\alpha\beta\gamma\delta,1})^{2N\rho_{ijkl}^{\alpha\beta\gamma\delta}} \prod_{ik} (\bar{\rho}^{\alpha\gamma,1})^{-N\rho_{ik}^{\alpha\gamma}} \\ &\times \prod_{jk} (\bar{\rho}_{jk}^{\beta\gamma,1})^{-N\rho_{jk}^{\beta\gamma}} \prod_{il} (\bar{\rho}_{il}^{\alpha\delta,1})^{-N\rho_{il}^{\alpha\delta}} \prod_{jl} (\bar{\rho}_{jl}^{\beta\delta,1})^{-N\rho_{jl}^{\beta\delta}}, \end{aligned} \quad (29)$$

where $\{\bar{\rho}_{ijkl}^{\alpha\beta\gamma\delta,1}\}$ represents the tetrahedron probability distribution corresponding to the equilibrium state of a defect-free bcc crystal (i.e., of the bulk configuration) which is equivalent to domain I (the same for its counterpart belonging to domain II, $\{\bar{\rho}_{ijkl}^{\alpha\beta\gamma\delta,II}\}$). The corresponding subcluster probabilities are obtained from $\{\bar{\rho}_{ijkl}^{\alpha\beta\gamma\delta,1}\}$ by the use of the reduction relations, already introduced.

With the definition of Ω_{ijkl} , P^I and P^{II} , Eq. (25) may now be rewritten as

$$\begin{aligned} \frac{\sigma^{(uvw)\{001\}}A}{Nk_B T} &= 2 \sum_{ijkl} \rho_{ijkl}^{\alpha\beta\gamma\delta} \ln \rho_{ijkl}^{\alpha\beta\gamma\delta} + \frac{1}{2} \sum_i \rho_i^\alpha \ln \rho_i^\alpha + \frac{1}{2} \sum_j \rho_j^\beta \ln \rho_j^\beta + \frac{1}{2} \sum_k \rho_k^\gamma \ln \rho_k^\gamma + \frac{1}{2} \sum_l \rho_l^\delta \ln \rho_l^\delta - \sum_{ik} \rho_{ik}^{\alpha\gamma} \ln \rho_{ik}^{\alpha\gamma} \\ &- \sum_{jk} \rho_{jk}^{\beta\gamma} \ln \rho_{jk}^{\beta\gamma} - \sum_{il} \rho_{il}^{\alpha\delta} \ln \rho_{il}^{\alpha\delta} - \sum_{jl} \rho_{jl}^{\beta\delta} \ln \rho_{jl}^{\beta\delta} - 2 \sum_{ijkl} \rho_{ijkl}^{\alpha\beta\gamma\delta} \ln \check{\rho}_{ijkl}^{\alpha\beta\gamma\delta} - \frac{1}{2} \sum_i \rho_i^\alpha \ln \check{\rho}_i^\alpha - \frac{1}{2} \sum_j \rho_j^\beta \ln \check{\rho}_j^\beta \\ &- \frac{1}{2} \sum_k \rho_k^\gamma \ln \check{\rho}_k^\gamma - \frac{1}{2} \sum_l \rho_l^\delta \ln \check{\rho}_l^\delta + \sum_{jk} \rho_{jk}^{\beta\gamma} \ln \check{\rho}_{jk}^{\beta\gamma} + \sum_{ik} \rho_{ik}^{\alpha\gamma} \ln \check{\rho}_{ik}^{\alpha\gamma} \\ &+ \sum_{il} \rho_{il}^{\alpha\delta} \ln \check{\rho}_{il}^{\alpha\delta} + \sum_{jl} \rho_{jl}^{\beta\delta} \ln \check{\rho}_{jl}^{\beta\delta} + \frac{\lambda}{k_B T} \left(1 - \sum_{ijkl} \rho_{ijkl}^{\alpha\beta\gamma\delta}\right), \end{aligned} \quad (30)$$

where λ is a new Lagrange multiplier introduced to take into account the constraint of normalization of the tetrahedron cluster probabilities in the layer, and $\check{\rho}_m^\xi \equiv (\check{\rho}_r^{\xi, I} \check{\rho}_r^{\xi, II})^{1/2}$ is a short notation for the square root of product of the bulk probability for configuration “ r ” of cluster ξ in domains I and II. Their particular expressions depend upon the choice of the defect’s APB vector ($\langle uvw \rangle$).

In the case of an $a_0^{A2}\langle 100 \rangle \{001\}$ APB, for example, the sublattices at both domains are related such that an α sublattice at domain (I) corresponds to a β sublattice in domain II, as well as a γ sublattice at domain (I) corresponds to a δ sublattice in domain II, and vice versa (schematically written as $\alpha \leftrightarrow \beta$ and $\gamma \leftrightarrow \delta$). This leads to

$$\check{\rho}_{i'}^\alpha = \check{\rho}_{i'}^\beta = (\rho_{i'}^\alpha \rho_{i'}^\beta)^{1/2}, \quad (31a)$$

$$\check{\rho}_{i'}^\gamma = \check{\rho}_{i'}^\delta = (\rho_{i'}^\gamma \rho_{i'}^\delta)^{1/2}, \quad (31b)$$

$$\check{\rho}_{i'j'}^{\alpha\gamma} = \check{\rho}_{i'j'}^{\beta\delta} = (\rho_{i'j'}^{\alpha\gamma} \rho_{i'j'}^{\beta\delta})^{1/2}, \quad (31c)$$

$$\check{\rho}_{i'j'}^{\beta\gamma} = \check{\rho}_{i'j'}^{\alpha\delta} = (\rho_{i'j'}^{\beta\gamma} \rho_{i'j'}^{\alpha\delta})^{1/2}, \quad (31d)$$

$$\check{\rho}_{i'j'k'l'}^{\alpha\beta\gamma\delta} = (\rho_{i'j'k'l'}^{\alpha\beta\gamma\delta} \rho_{i'j'k'l'}^{\alpha\beta\gamma\delta})^{1/2}. \quad (31e)$$

For the $\langle uvw \rangle = a_0^{A2}/2 \langle 111 \rangle$ case, on the other hand, the correspondence of sublattices at both domains can be schematically written as $\alpha \rightarrow \gamma \rightarrow \beta \rightarrow \delta \rightarrow \alpha$, leading to:

$$\check{\rho}_{i'}^\alpha = (\rho_{i'}^\alpha \rho_{i'}^\gamma)^{1/2}, \quad (32a)$$

$$\check{\rho}_{j'}^\beta = (\rho_{j'}^\beta \rho_{j'}^\delta)^{1/2}, \quad (32b)$$

$$\check{\rho}_{k'}^\gamma = (\rho_{k'}^\gamma \rho_{k'}^\beta)^{1/2}, \quad (32c)$$

$$\check{\rho}_{l'}^\delta = (\rho_{l'}^\delta \rho_{l'}^\alpha)^{1/2}, \quad (32d)$$

$$\check{\rho}_{i'k'}^{\alpha\gamma} = (\rho_{i'k'}^{\alpha\gamma} \rho_{i'k'}^{\beta\gamma})^{1/2}, \quad (32e)$$

$$\check{\rho}_{j'l'}^{\beta\gamma} = (\rho_{j'l'}^{\beta\gamma} \rho_{j'l'}^{\beta\delta})^{1/2}, \quad (32f)$$

$$\check{\rho}_{i'l'}^{\alpha\delta} = (\rho_{i'l'}^{\alpha\delta} \rho_{i'l'}^{\alpha\gamma})^{1/2}, \quad (32g)$$

$$\check{\rho}_{j'i'}^{\beta\delta} = (\rho_{j'i'}^{\beta\delta} \rho_{j'i'}^{\alpha\delta})^{1/2}, \quad (32h)$$

$$\check{\rho}_{i'j'k'l'}^{\alpha\beta\gamma\delta} = (\rho_{i'j'k'l'}^{\alpha\beta\gamma\delta} \rho_{i'j'k'l'}^{\alpha\beta\gamma\delta})^{1/2}. \quad (32i)$$

Minimising Eq. (30) with respect to $\rho_{ijkl}^{\alpha\beta\gamma\delta}$, one obtains

$$\begin{aligned} \frac{A}{Nk_B T} \frac{\partial \sigma^{\langle uvw \rangle \{001\}}}{\partial \rho_{ijkl}^{\alpha\beta\gamma\delta}} &\equiv \exp \left\{ \frac{\lambda}{2k_B T} \right\} + 2 \ln(\rho_{ijkl}^{\alpha\beta\gamma\delta}) \\ &+ \frac{1}{2} \ln(\rho_i^\alpha \rho_j^\beta \rho_k^\gamma \rho_l^\delta) - \ln(\rho_{ik}^{\alpha\gamma} \rho_{jk}^{\beta\gamma} \rho_{il}^{\alpha\delta} \rho_{jl}^{\beta\delta}) \\ &- 2 \ln(\check{\rho}_{ijkl}^{\alpha\beta\gamma\delta}) - \frac{1}{2} \ln(\check{\rho}_i^\alpha \check{\rho}_j^\beta \check{\rho}_k^\gamma \check{\rho}_l^\delta) \end{aligned}$$

$$\begin{aligned} &+ \ln(\check{\rho}_{ik}^{\alpha\gamma} \check{\rho}_{jk}^{\beta\gamma} \check{\rho}_{il}^{\alpha\delta} \check{\rho}_{jl}^{\beta\delta}) \\ &= 0. \end{aligned} \quad (33)$$

C. Application of the NIM to the SP-CVM “layer” formulation

We introduce the auxiliary variables $\Xi_{i,j,k,l}^{\alpha\beta\gamma\delta}$

$$\Xi_{ijkl}^{\alpha\beta\gamma\delta} = \rho_{ijkl}^{\alpha\beta\gamma\delta} \frac{(\check{\rho}_i^\alpha \check{\rho}_j^\beta \check{\rho}_k^\gamma \check{\rho}_l^\delta)^{1/4}}{(\check{\rho}_{ik}^{\alpha\gamma} \check{\rho}_{jk}^{\beta\gamma} \check{\rho}_{il}^{\alpha\delta} \check{\rho}_{jl}^{\beta\delta})^{1/2}} \frac{(\rho_{ik}^{\alpha\gamma} \rho_{jk}^{\beta\gamma} \rho_{il}^{\alpha\delta} \rho_{jl}^{\beta\delta})^{1/2}}{(\rho_i^\alpha \rho_j^\beta \rho_k^\gamma \rho_l^\delta)^{1/4}}. \quad (34)$$

Before starting the first iteration of the algorithm, the initial value of $\Xi_{ijkl}^{\alpha\beta\gamma\delta}$ is chosen by setting

$$\Xi_{ijkl}^{\alpha\beta\gamma\delta} \approx \check{\rho}_{ijkl}^{\alpha\beta\gamma\delta}. \quad (35)$$

After the first iteration, the Lagrange multiplier and a new set of probabilities are calculated using the normalization constraint

$$\lambda = k_B T \ln \left(\sum_{i,j,k,l} \Xi_{i,j,k,l}^{\alpha\beta\gamma\delta} \right), \quad (36a)$$

$$\rho_{i,j,k,l}^{\alpha\beta\gamma\delta} = \frac{\Xi_{i,j,k,l}^{\alpha\beta\gamma\delta}}{\sum_{i,j,k,l} \Xi_{i,j,k,l}^{\alpha\beta\gamma\delta}}. \quad (36b)$$

The subcluster probabilities are then calculated from this new probability set using the reduction relations and substituted into Eq. (34).

With the repeated application of the algorithm, the set $\{\rho_{i,j,k,l}^{\alpha\beta\gamma\delta}\}$ converges to a fixed point in the tetrahedron probability space, which corresponds to a minimum of the surface tension. After the minimum has been found, the surface tension can be easily obtained through the Lagrange multiplier λ as

$$\sigma^{\langle uvw \rangle \{001\}} A = \lambda. \quad (37)$$

III. APPLICATION TO THE bcc FE-AL SYSTEM

The CVM formalism used in the present work for the bulk calculations in the bcc Fe-Al system using the IT cluster approximation has been thoroughly outlined in several previous publications by one of the present authors,^{23,24,34,35} and shall not be reproduced here. For the sake of completeness only the main aspects of the Bulk calculation will be briefly described.

The internal energy ($U^{(0)}$) of a bcc lattice with $N^{(0)}$ sites⁴¹ (containing $N^{\alpha\beta\gamma\delta} = 6N^{(0)}$ irregular tetrahedra) is written as²³

$$U^{(0)} = 6N^{(0)} \sum_{i,j,k,l=Fe,Al} \varepsilon_{ijkl}^{\alpha\beta\gamma\delta} \rho_{ijkl}^{\alpha\beta\gamma\delta}. \quad (38)$$

In this expression, $\varepsilon_{ijkl}^{\alpha\beta\gamma\delta}$ represents the eigenenergy⁴² associated with this configuration.

It has to be reminded that the eigenenergy matrix $\{\varepsilon_{ijkl}^{\alpha\beta\gamma\delta}\}$ is highly degenerate due to crystal symmetry constraints. Both configurations FeAlFeAl and AlFeAlFe, for example, represent a B32 FeAl stoichiometric compound, differing only by a translation of the origin of the lattice by lattice vector $a_0/2[111]$. Since the energy of the compound cannot depend on the choice of the origin for the reference lattice, it follows that $\varepsilon_{AlFeAlFe}^{\alpha\beta\gamma\delta} = \varepsilon_{FeAlFeAl}^{\alpha\beta\gamma\delta}$. The same is true for the two remaining degenerate configurations (FeAlAlFe and AlFeFeAl).

Set $\{\varepsilon_{ijkl}^{\alpha\beta\gamma\delta}\}$ (including the two reference values, $\varepsilon_{FeFeFeFe}^{\alpha\beta\gamma\delta} = \varepsilon_{AlAlAlAl}^{\alpha\beta\gamma\delta} = 0$) contains all information needed for the description of the system. It is a common practice in the literature, however, to further decompose the configuration eigenenergies into pair interactions (nearest and next-nearest neighbors), completing the set with higher-order cluster interactions. For the sake of compatibility with the literature the same criterion has been adopted in the present work, using

$$\varepsilon_{ijkl}^{\alpha\beta\gamma\delta} = \frac{1}{6}(w_{ik}^{(1)} + w_{il}^{(1)} + w_{jk}^{(1)} + w_{jl}^{(1)}) + \frac{1}{4}(w_{ij}^{(2)} + w_{kl}^{(2)}) + \tilde{w}_{ijkl}. \quad (39)$$

In Eq. (39), $w_{i'j'}^{(1)}$ and $w_{i'j'}^{(2)}$ represent, respectively, nearest and next-nearest pair interactions, with fractions $\frac{1}{6}$ and $\frac{1}{4}$ correcting for the right number of pair clusters in the set of 6N tetrahedra. Term \tilde{w}_{ijkl} represents an “excess” interaction, containing the contributions to $\varepsilon_{ijkl}^{\alpha\beta\gamma\delta}$ which cannot be ascribed to pair interactions. Following Schön and Inden,²³ the set $\varepsilon_{ijkl}^{\alpha\beta\gamma\delta}$ will be rewritten in terms of interactions $w_{FeAl}^{(1)}$, $w_{FeAl}^{(2)}$, $\tilde{w}_{FeAlFeAl}$, and $\tilde{w}_{FeAlAlAl}$. This choice of parameters is arbitrary and other ways of decomposing $\varepsilon_{ijkl}^{\alpha\beta\gamma\delta}$ are possible (see for example Ref. 36), but this is irrelevant for the present discussion and for the thermodynamic description of the system.

The entropy, $S^{(0)}$, of the bulk system will be given by³⁵

$$\begin{aligned} S^{(0)} = -N^{(0)}k_B \left[6 \sum_{ijkl} \bar{\rho}_{ijkl}^{\alpha\beta\gamma\delta} \ln \bar{\rho}_{ijkl}^{\alpha\beta\gamma\delta} - 3 \sum_{ijk} (\bar{\rho}_{ijk}^{\alpha\beta\gamma} \ln \bar{\rho}_{ijk}^{\alpha\beta\gamma} \right. \\ + \bar{\rho}_{ijk}^{\alpha\beta\delta} \ln \bar{\rho}_{ijk}^{\alpha\beta\delta} + \bar{\rho}_{ijk}^{\alpha\gamma\delta} \ln \bar{\rho}_{ijk}^{\alpha\gamma\delta} + \bar{\rho}_{ijk}^{\beta\gamma\delta} \ln \bar{\rho}_{ijk}^{\beta\gamma\delta}) \\ + \frac{3}{2} \sum_{ij} (\bar{\rho}_{ij}^{\alpha\beta} \ln \bar{\rho}_{ij}^{\alpha\beta} + \bar{\rho}_{ij}^{\gamma\delta} \ln \bar{\rho}_{ij}^{\gamma\delta}) + \sum_{ij} (\bar{\rho}_{ij}^{\alpha\gamma} \ln \bar{\rho}_{ij}^{\alpha\gamma} \\ + \bar{\rho}_{ij}^{\alpha\delta} \ln \bar{\rho}_{ij}^{\alpha\delta} + \bar{\rho}_{ij}^{\beta\gamma} \ln \bar{\rho}_{ij}^{\beta\gamma} + \bar{\rho}_{ij}^{\beta\delta} \ln \bar{\rho}_{ij}^{\beta\delta}) \\ \left. - \frac{1}{4} \sum_i (\bar{\rho}_i^\alpha \ln \bar{\rho}_i^\alpha + \bar{\rho}_i^\beta \ln \bar{\rho}_i^\beta + \bar{\rho}_i^\gamma \ln \bar{\rho}_i^\gamma + \bar{\rho}_i^\delta \ln \bar{\rho}_i^\delta) \right]. \quad (40) \end{aligned}$$

With the help of Eqs. (38) and (40), we write the CVM free energy functional, Z^*

TABLE I. Interaction parameters (in $k_B K = 8.3145$ J/mol $= 8.617 \times 10^{-5}$ eV/atom units) used for the thermodynamic description of the bcc Fe-Al system (Ref. 23).

$w_{FeAl}^{(1)}$	$w_{FeAl}^{(2)}$	$\tilde{w}_{FeAlFeAl}$	$\tilde{w}_{FeAlAlAl}$
-840	-370	+35.1	0.0

$$\begin{aligned} Z^*(T, \mu_i^*) = F^{(0)} - \sum_{i=Fe,Al} \mu_i^* x_i = U^{(0)} - TS^{(0)} + \\ - \sum_{i,j,k,l=Fe,Al} \left(\frac{\mu_i^* + \mu_j^* + \mu_k^* + \mu_l^*}{4} \right) \bar{\rho}_{i,j,k,l}^{\alpha\beta\gamma\delta}, \quad (41) \end{aligned}$$

where μ_i^* and x_i represent the chemical potential in the “baricentric” reference state (see Eleno and Schön³⁵) and the molar fraction of component i in the alloy. The functional Z^* is then minimized with respect to $\bar{\rho}_{i,j,k,l}^{\alpha\beta\gamma\delta}$ (e.g., using the NIM algorithm, already introduced) for given values of T and μ_i^* . The set $\{\bar{\rho}_{i,j,k,l}^{\alpha\beta\gamma\delta}\}$ which minimizes the functional corresponds to the probability distribution of the equilibrium bulk configuration, which is then used as a constant in Eqs. (31) and (32) and substituted into the minimization algorithm of the SP-CVM method [Eq. (35)].

Table I presents the interaction parameters used in the present calculation. These parameters have been derived in a previous work by one of the authors²³ by fitting experimental data on the order-disorder equilibria obtained from the literature (see Inden and Pepperhof,³⁷ and references therein).

The “thermal” APB energy calculations are presented here for two isotherms: $T = 1000$ K (Fig. 3), since at this temperature the agreement between calculated values of aluminum activity and those obtained in an independent experimental investigation²⁷ is optimal (see Schön and Inden²⁴); and $T = 623$ K (Fig. 4), which corresponds to the estimated temperature for vacancy “freezing” in Fe-Al alloys.³⁸ In both cases the investigated composition range is limited to alloys with $x_{Al} \leq 0.5$, since the bcc-based superlattices are no longer

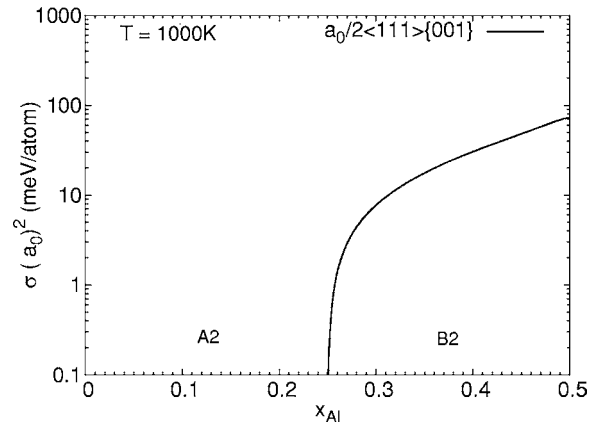


FIG. 3. “Thermal” APB energy for the $a_0^2/2\langle 111 \rangle \{001\}$ defect at the $T = 1000$ K, as calculated by the SP-CVM “layer” formulation.

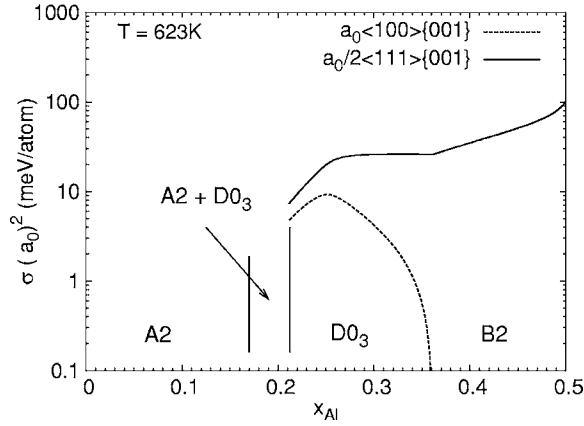


FIG. 4. “Thermal” APB energy for the $a_0^{A2}\langle 100 \rangle \{001\}$ and $a_0^{A2}/2\langle 111 \rangle \{001\}$ defects at the $T=623$ K, as calculated by the SP-CVM “layer” formulation.

stable for Al-richer alloys. Both isotherms have also been used in previous “mechanical” APB energy calculations using BC-CVM by the present authors.^{4,9}

IV. DISCUSSION

The proof of Eq. (1), here deduced for the case of $\{001\}$ APBs (with a layer composed of two atom planes) is, in fact, valid for layers composed by any number of planes. To prove this, we observe that the critical point in the deduction, which defines the form of Eq. (1), is the expression for the system’s entropy in the layer pair approximation [Eq. (6)]. This expression is deduced based on its topological equivalence with the unidimensional (1D) lattice in the pair approximation, and this equivalence does not depend on the number of atom planes composing the layer. An extension to a cluster approximation beyond the layer pair in 1D lattices is not necessary since the obtained entropy expression¹⁴ is identical to the one derived from the exact solution of the Ising model.³⁹

The extension of the formalism also results in an unexpected advantage over the previous formulations of the SP-CVM method. These formulations, when applied to 3D lattices, were always based on the subdivision of the system into atom planes, i.e., 2D clusters. Correlations of a 3D lattice cannot be correctly described by a 2D cluster and this leads to the introduction of additional constraint terms in the free-energy expression to take into account the correlations between two neighboring planes (the so-called “out-of-plane” correlations). The Lagrange multipliers corresponding to these constraint terms have to be determined for each iteration of the NIM. This determination is done by a separate NIM-based self-consistent algorithm. This leads to the introduction of the so-called *minor iterations* of the NIM (see, for example, Kikuchi¹⁹ and Cenedese and Kikuchi¹¹). The layers, being formed by two or more atom planes, are necessarily 3D clusters and the interplanar correlations are trivially taken care of by the constraint term defined in Eq. (8). This produces a more compact (and consequently faster) algorithm. This is a property of the layer formalism, since the

layer can always be defined as a large enough set of atom planes (see above) such that all relevant out-of-plane correlations (defined by the basic cluster chosen for the implementation) are contained in the intersection of two neighboring layers.

Figure 3 shows the variation of the thermal APB energy for the $a_0^{A2}/2\langle 100 \rangle \{001\}$ APB at the $T=1000$ K isotherm. At this temperature and composition range only the B2 superlattice and the disordered bcc phases are stable. In both structures the α sublattices are crystallographically equivalent to the β ones (as well as the γ sublattices being equivalent to the δ ones); thus, the $a_0^{A2}\langle 100 \rangle$ vector does not produce an APB. Comparing with the previous results on “mechanical” APBs,^{4,9} one observes that in both cases the APB energy presents a maximum at the ideal stoichiometric ratio of the B2 FeAl phase ($x_{Al}=0.5$), but that its decrease, when approaching the second-order B2/A2 boundary, is much more pronounced in the case of the thermal APBs. Mechanical APBs are able to exist even in the disordered lattice [in the form of “diffuse” APBs (Refs. 1,8)], since the constrained equilibrium imposes a discontinuity in the configuration gradient at the interface even when the distinction between the sublattices vanishes. This leads to nonzero values for the mechanical APB energy at the second-order boundary, and this variable tends toward zero only in the limit of infinite dilution.^{4,9} In thermal APBs, on the contrary, local equilibrium is attained at the interface and the configuration gradient must be, therefore, continuous. The thermal APB energy must thus tend towards zero at the second-order boundary, where the distinction between the domains vanishes [this can be easily proven by setting $p^I(\mu)=p^{II}(\mu)$ in Eq. (1)].

Figure 4 shows the variation of the APB energies for defects with APB vectors $a_0^{A2}/2\langle 111 \rangle$ and $a_0^{A2}\langle 100 \rangle$ at the 623 K isotherm. As expected, the APB energy of the $a_0^{A2}\langle 100 \rangle$ defect is positive inside the stability field of the $D0_3$ phase, vanishing at the $D0_3/B2$ second-order boundary as the aluminum content of the alloy is increased. This defect presents a maximum point at the ideal stoichiometric ratio of the $D0_3$ phase ($x_{Al}=0.25$) and presents a nonzero value at the border of the two-phase field for the $A2+D0_3$ heterogeneous equilibrium, in agreement with the first-order character of this transformation. The composition dependence of the APB energy for the $a_0^{A2}/2\langle 111 \rangle$ defect is more complex when compared with the 1000 K isotherm: the maximum at the ideal stoichiometric ratio of the B2 phase is more pronounced and a contribution of the ordering in the $D0_3$ field (which is due to an increase in the number of unlike bonds in the $\gamma\delta$, i.e., next-nearest neighbor pairs) counteracts the decrease tendency due to loss of unlike bonds between nearest-neighbor pairs, leading to an almost constant value for the APB energy in the composition range $0.27 \leq x_{Al} \leq 0.36$.

V. CONCLUSIONS

The scalar product-cluster variation method for the calculations of thermal antiphase boundary energies has been applied to the case of $\{001\}$ APBs in body-centered cubic lattices in two different cases, corresponding to APB vectors

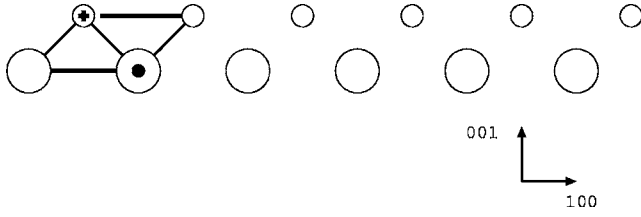


FIG. 5. Projection of a (001) layer of a bcc crystal along lattice direction $[0\bar{1}0]$. Large circles represent atoms located at cube vertices and small circles to atoms located at cube centers (or vice versa). Two adjacent IT clusters are represented in the figure, where thin lines correspond to nearest neighbors (nn) and thick lines to next-nearest neighbors (nnn). Symbol “+” corresponds to a nnn bond along lattice direction $a_0[010]$ and “●” to a nnn bond along lattice direction $a_0[0\bar{1}0]$ (i.e., both are perpendicular to the plane of the figure).

$a_0^{A2}\langle 100 \rangle$ and $a_0^{A2}/2\langle 111 \rangle$, respectively. This required the introduction of the concept of “layer” and the corresponding extension of the proof for the SP-CVM to address this case. As a consequence, two major conclusions can be drawn from the structure of the proof:

The present proof is valid for layers containing an arbitrary number of atom planes, and

The new formalism does not require additional minimization steps (*minor* iterations) to obtain the defect’s surface tension. The formalism has been applied to the case of nonmagnetic bcc Fe-Al alloys at two isotherms, 1000 and 623 K. The variation of the thermal APB surface tensions with composition in this system shows that, unlike the case of the mechanical APBs, the thermal APBs vanish at second-order boundaries.

ACKNOWLEDGMENTS

This work was initiated during Professor Kikuchi’s visit to Brazil, back in the year 2000. Sadly he passed away before seeing this finished manuscript. The many valuable lessons he taught me (C.G.S.), as well as his generous friendship, are gratefully acknowledged. C.G.S. wishes to thank Professor Dr. J. W. Cahn for encouragement and for valuable advice. This work has been partially supported by the São Paulo State Research Funding Agency (FAPESP, São Paulo-SP, Brazil) under Grants 99/07986-0 and 99/07570-8, and by the Brazilian National Research Council (CNPq, Brasilia-DF, Brazil) under Grant 301393/2004-8.

APPENDIX: DERIVATION OF THE LAYER CONFIGURATIONAL ENTROPY

Figure 5 presents a projection of the single (001) layer along lattice vector $[0\bar{1}0]$. We define here the multiplicity of

TABLE II. Multiplicities of the basic cluster and of its subclusters in a (001) layer of a bcc crystal containing N atoms.

Subcluster (ξ)	$q^{\xi}N$
Point	$2N$
nn Pair	$4N$
nnn Pair	$4N$
Triangle	$8N$
IT	$2N$

a subcluster ξ , q^{ξ} , as the number of subclusters sharing a common lattice point of the bcc lattice. The multiplicities of the IT cluster and of its subclusters (triangle, next-nearest neighbor pair, nearest-neighbor pair, and point) are obtained by inspection of Fig. 5 and are presented in Table II.

Using these multiplicities, the configurational entropy of the layer, S_{ℓ} , may be expressed as³²

$$\exp\left[\frac{S_{\ell}}{k_B}\right] = (W_{\text{point}})^2 (G_{\text{nn pair}})^4 (G_{\text{nnn pair}})^4 (G_{\text{triangle}})^8 (G_{\text{IT}})^2, \quad (\text{A1})$$

where W_{point} represents the number of configurations of a disjoint set of N points

$$W_{\text{point}} = \frac{N!}{\{\text{point}\}_N} \equiv \frac{N!}{\{\alpha\}_N^{1/4} \{\beta\}_N^{1/4} \{\gamma\}_N^{1/4} \{\delta\}_N^{1/4}}. \quad (\text{A2})$$

In the expression above, use was made of the simplified notation for products of factorials of numbers of clusters, introduced in Sec. II [Eq. (28)].

Variables G_{ξ} in Eq. (A1) represent the correlation correction functions (CCF) for subcluster ξ , previously introduced by one of the present authors.³² The CCFs for the subclusters of the tetrahedron are reproduced below

$$G_{\text{nnPair}} = \frac{\{\text{point}\}_N^2}{N! \{\text{nn pair}\}_N}, \quad (\text{A3a})$$

$$G_{\text{nnnPair}} = \frac{\{\text{point}\}_N^2}{N! \{\text{nnn pair}\}_N}, \quad (\text{A3b})$$

$$G_{\text{Triangle}} = \frac{N! \{\text{nn pair}\}_N^2 \{\text{nnn pair}\}_N}{\{\text{point}\}_N^3 \{\text{triangle}\}_N}, \quad (\text{A3c})$$

$$G_{\text{IT}} = \frac{\{\text{point}\}_N^4 \{\text{triangle}\}_N^4}{N! \{\text{nn pair}\}_N^4 \{\text{nnn pair}\}_N^2 \{\text{IT}\}_N}. \quad (\text{A3d})$$

Substituting Eqs. (A2) and (A3a)–(A3d) into Eq. (A1), one obtains Eq. (27).

*Electronic address: schoen@usp.br

- ¹F. Král, Dr. rer. nat. dissertation, ETH-Zürich, Diss. ETH Nr. 11685, Zürich, Switzerland, 1996).
- ²F. Král, P. Schwander, and G. Kostorz, *Acta Mater.* **45**, 675 (1997).
- ³F. J. G. Landgraf, M. Emura, J. C. Teixeira, and M. F. de Campos, *J. Magn. Magn. Mater.* **215–216**, 97 (2000).
- ⁴C. G. Schön and R. Kikuchi, *Z. Metallkd.* **89**, 868 (1998).
- ⁵A. Bieber and F. Gautier, *Z. Phys. B: Condens. Matter* **57**, 335 (1984).
- ⁶P. A. Flinn, *Trans. Metall. Soc. AIME* **218**, 145 (1960).
- ⁷G. Inden, S. Bruns, and H. Ackermann, *Philos. Mag. A* **53**, 87 (1986).
- ⁸F. Král, P. Schwander, G. Schönfeld, and G. Kostorz, *Mater. Sci. Eng., A* **234–236**, 351 (1997).
- ⁹C. G. Schön and R. Kikuchi, *Theor. Appl. Fract. Mech.* **35**, 243 (2001).
- ¹⁰R. Kikuchi and J. W. Cahn, *J. Phys. Chem. Solids* **23**, 137 (1962).
- ¹¹P. Cenedese and R. Kikuchi, *J. Phys. I* **7**, 255 (1996).
- ¹²W. A. Oates, H. Wenzl, and T. Mohri, *CALPHAD: Comput. Coupling Phase Diagrams Thermochem.* **20**, 37 (1996).
- ¹³K. Hack, *The SGTE Casebook: Thermodynamics at Work*, Materials Modeling Series (The Institute of Metals, London, UK, 1996).
- ¹⁴R. Kikuchi, *Phys. Rev.* **81**, 988 (1951).
- ¹⁵R. Kikuchi and J. W. Cahn, *Acta Metall.* **27**, 1337 (1979).
- ¹⁶R. Kikuchi, *J. Chem. Phys.* **57**, 777 (1972).
- ¹⁷R. Kikuchi, *J. Chem. Phys.* **57**, 783 (1972).
- ¹⁸R. Kikuchi, *J. Chem. Phys.* **52**, 787 (1972).
- ¹⁹R. Kikuchi, *J. Chem. Phys.* **65**, 4545 (1976).
- ²⁰G. W. Woodbury, *J. Chem. Phys.* **51**, 1231 (1969).
- ²¹G. W. Woodbury, *J. Chem. Phys.* **53**, 3728 (1970).
- ²²D. B. Clayton and G. W. Woodbury, *J. Chem. Phys.* **55**, 3895 (1971).
- ²³C. G. Schön and G. Inden, *J. Chim. Phys. Phys.-Chim. Biol.* **94**, 1143 (1997).
- ²⁴C. G. Schön and G. Inden, *Acta Mater.* **46**, 4219 (1998).
- ²⁵C. G. Schön and G. Inden, *J. Magn. Magn. Mater.* **232**, 209 (2001).
- ²⁶C. G. Schön and G. Inden, *J. Magn. Magn. Mater.* **234**, 520 (2001).
- ²⁷H. Kleykamp and H. Glasbrenner, *Z. Metallkd.* **88**, 230 (1997).
- ²⁸C. G. Schön, Dr. rer. nat. dissertation, Universität Dortmund, Germany, 1998.
- ²⁹R. Kikuchi, *J. Chem. Phys.* **60**, 1071 (1974).
- ³⁰M. Pretti, *J. Stat. Phys.* **119**, 659 (2005).
- ³¹G. Inden and W. Pitsch, *Atomic Ordering* Vol. 5 of Materials Science and Technology (VCH, Weinheim, Germany, 1991), Chap. 9, pp. 497–552.
- ³²R. Kikuchi, *Prog. Theor. Phys. Suppl.* **115**, 1 (1994).
- ³³R. Kikuchi, *J. Chem. Phys.* **66**, 3352 (1977).
- ³⁴C. G. Schön, *J. Phase Equilib.* **22**, 287 (2001).
- ³⁵L. T. F. Eleno and C. G. Schön, *CALPHAD: Comput. Coupling Phase Diagrams Thermochem.* **27**, 335 (2003).
- ³⁶R. McCormack, D. de Fontaine, C. Wolverton, and G. Ceder, *Phys. Rev. B* **51**, 15808 (1995).
- ³⁷G. Inden and W. Pepperhoff, *Z. Metallkd.* **81**, 770 (1990).
- ³⁸J. Herrmann, G. Inden, and G. Sauthoff, *Acta Mater.* **51**, 2847 (2003).
- ³⁹E. Ising, *Z. Phys.* **31**, 253 (1925).
- ⁴⁰As in the previous publications by the authors (Refs. 4,9), the following convention will be adopted in the present work: Roman indices correspond to species, while Greek indices correspond to lattice positions and related variables (e.g., lattice points, clusters, and subclusters).
- ⁴¹For the sake of compatibility with the notation introduced in Sec. II A, a superscript “(0)” is introduced here to denote variables obtained in the bulk calculation.
- ⁴²The formalism used in the present work is formally equivalent to the Ising model of statistical mechanics. In this sense the eigenenergies defined above are to be understood as the eigenvalues of the Hamilton operator of the Ising model for the given configuration (see Schön and Inden, Ref. 25).